SAND99-1914J

Oxygen Implant Isolation of n-GaN Field-Effect Transistor Structures

G. Dang[(1)], X. A. Cao[(2)], F. Ren[(1)], S. J. Pearton[(2)], J. Han[(3)], A. G. Baca[(3)], and R. J. Shul[(3)]

(1) Department of Chemical Engineering, University of Florida, Gainesville FL 32611 USA

(2) Department of Materials Science and Engineering, University of Florida, Gainesville FL 32611 USA

(3) Sandia National Laboratories, Albuquerque NM 87185 USA

Abstract

Multiple-energy (30-325 keV) O^+ implantation into GaN field-effect transistor structures (n ~10^{18} cm^{-3}, 3000 Å thick) can produce as-implanted sheet resistances of $4x10^{12}$ Ω/□, provided care is taken to ensure compensation of the region up to the projected range of the lowest energy implant. The sheet resistance remains above 10^7 Ω/□ to annealing temperatures of ~650° C and displays an activation energy of 0.29 eV. No diffusion of the implanted oxygen was observed for anneals up to 800° C.

Introduction

Implant isolation has been widely used in compound semiconductor devices for inter-device isolation such as in transistor circuits or to produce current channeling such as in lasers.[1-3] The implantation process can compensate the semiconductor layer either by a damage or chemical mechanism, maintaining a planar device morphology without the need for etched mesa isolation. For damage compensation, the resistance typically goes through a maximum with increased post-implantation annealing temperature as the damage is annealed out and hopping conduction is reduced. At higher temperatures the defect density is further reduced below that required to compensate the material and the resistivity decreases. For chemical compensation, the post-implantation resistance again increases with annealing temperature with a reduction in hopping conduction but it then stabilizes at higher temperatures as a thermally stable compensating deep level is formed. Typically there is a minimum dose (dependent on the doping level of the sample) required for the chemically active isolation species to achieve thermally stable compensation.[4] Thermally stable implant isolation has been reported for n- and p-type AlGaAs where an Al-O complex is thought to form[4,5] and for C-doped GaAs and AlGaAs where a C-N complex is postulated.[6]

N-implantation (at doses of 10^{12}-10^{13} cm^{-3}) effectively compensates both p- and n-type GaN.[7-9] For both doping types, the resistance first increases with annealing temperature then reaches a maximum before demonstrating a significant reduction in resistance after a 850° C anneal for n-type and a 950° C anneal for p-type GaN. This behavior is typical of implant-damage compensation. The defect levels in this N-implanted material estimated from Arrhenius plots of the resistance/temperature product are 0.83 eV for initially n-type and 0.90 eV for initially p-type GaN. These levels are still not at mid-gap, but are sufficiently deep to realize a sheet resistance $>10^9\ \Omega/\square$. He implantation has also been reported to effectively isolate n-type GaN(7), with the material remaining compensated to over 850° C. Interestingly, H-implanted compensation of n-type GaN is reported to anneal out at ~400° C(7) with an anomalous dependence on implant energy. The reason for this is presently not known. In light of this result however, H-implantation in GaN will require further study, as H is often the ion of choice for photonic device isolation applications that require deep isolation schemes. Moreover, both the He and N isolation appear to rely solely on implantation damage without any chemical compensation effects analogous to those in the O/AlGaAs case.(1, 4, 5) However, the implantation-induced defects in GaN are more thermally stable than other III-V semiconductor materials, such as GaAs or InP, where the damage levels begin to anneal out below 700° C.(1) This may be a result of the higher bandgap of GaN or the more polar nature of the lattice causing more stable defects.

Implant isolation of the In-containing nitrides (InN, InGaN and InAlN) was first reported using F-implantation.(8) That work showed that InN did not demonstrate significant compensation while the ternaries increased in sheet resistance by roughly an order-of-magnitude after a 500° C anneal. Data from a more extensive study of $In_xGa_{1-x}N$ implant isolation for varying In-composition using N- and F-implantation showed that InGaN ternaries only realize a maximum of a 100 fold increase in sheet resistance independent of ion species after a 500° C anneal. Pure InN shows a higher increase of 3 orders-of-magnitude but still only achieves a maximum sheet resistance of $10^4\ \Omega/\square$. This may be high enough for some photonic device current-guiding applications but is not sufficient for inter-device isolation in electronic circuits. The damage levels created by N-implantation are estimated from an Arrhenius plot of the resistance/temperature product to be a maximum of 390 meV below the conduction band.[9] The defect level is high in the energy gap, not near mid-gap as is ideal for implant compensation. The position of the damage level is analogous to the defect position reported for implant compensated n-type InP and InGaAs[10] but different from the damage-associated, mid-gap states created in GaAs and AlGaAs.[4, 5]

InAlN, in contrast to InGaN, can be highly compensated with N- or O-implantation with over a three order-of-magnitude increase in sheet resistance after a 600-700° C anneal while F-implantation produces only one order-of-magnitude increase in sheet resistance.[8,11] The compensating level in InAlN is also high in the bandgap with the deepest level estimated from Arrhenius plots as being 580 meV below the conduction band edge in high dose N-isolated material, however it is sufficiently deep to achieve highly compensated material.[11] The enhanced compensation for N- and O-implantation, as compared to F-implantation in InAlN, suggests some chemical component to the compensation process. For N-implantation a reduction in N-vacancies, that are thought to play a role in the as-grown n-type conduction, may explain the enhanced compensation. For O-implantation, the enhanced compensation may be the result of the formation of an Al-O complex as is thought to occur in O-implanted AlGaAs.[5,6]

The recent emphasis in developing GaN electronics for high power, high temperature applications means there is a need to achieve effective device isolation processes using implantation. Very effective isolation of AlGaN/GaN heterostructure field effect transistor (HFET) structures has been achieved using a combined P^+/He^+

implant process.[12] The groups of Asbeck and Lau at UCSD demonstrated that a dual energy (75/180 keV) P^+ implant (doses of $5x10^{11}$ and $2x10^{12}$ cm^{-2}, respectively), followed by a 75 keV He^+ implant ($6x10^{13}$ cm^{-2}) was able to produce a sheet resistance of $\sim 10^{12}$ $\Omega/\square$ in AlGaN/GaN structures with 1 μm thick undoped GaN buffers. The temperature dependence of the resistivity showed an activation energy of 0.71 eV[13],consistent with past measurements of deep states induced in GaN by implant damage.[14]

In this paper we report on the creation of very high resistance $\sim 4x10^{12}$ $\Omega/\square$ regions in n-GaN by O implantation. The resistance stays above 10^9 $\Omega/\square$ for annealing to ~500 °C and to measurement temperatures of ~200 °C.

Experimental

The layer structure shown in Figure 1 was grown on c-plane Al_2O_3 substrates by rf plasma-assisted Molecular Beam Epitaxy.[15] The uppermost n-GaN was Si-doped to produce a carrier concentration of $\sim 10^{18}$ cm^{-3}. This structure simulates a GaN metal semiconductor field effect transistor (MESFET) or metal-oxide semiconductor FET (MOSFET) layer design. In some structures, 490 Å of Ti was deposited by e-beam evaporation on top of the GaN, and the implant performed through that layer. This procedure enabled us to achieve better near-surface isolation properties. The implant scheme consisted of 5 different conditions, i.e. O^+ ions implanted at the following doses and energies: 30 keV, $3x10^{12}$ cm^{-2}; 60 keV, $5x10^{12}$ cm^{-2}; 125 keV, $9x10^{12}$ cm^{-2}; 200 keV, $9x10^{12}$ cm^{-2} and 325 keV, $2x10^{13}$ cm^{-2}. The total O^+ dose was therefore $4.6x10^{13}$ cm^{-2}. The ion profiles were simulated by P-CODE™, while the displacement damage was simulated by the Transport-of-Ions-In-Matter (TRIM) code. The sheet resistance was obtained from Transmission Line Measurements (TLM) using Ti/Au contacts alloyed at 800 °C prior to the implantation step.

Results and Discussion

Figure 2 shows the calculated ion profiles for the multiple-energy O^+ implant scheme into bare GaN. Note that there is a region at the immediate surface (≤250 Å) that has a much lower ion concentration, simply because the projected range of the 30 keV O^+ ions is ~300 Å. It is important to know the expected atom displacement density in this surface region, because it is the ion damage that actually produces the high resistance behavior in implanted semiconductors.(1)

The vacancy concentration profile calculated from the nuclear stopping energy deposition by the implanted O^+ ions is shown in Figure 3. This also shows that the near-surface region does receive as much cumulative damage as the region from 250-3000 Å. Adequate coverage of this near-surface region is a common problem in implant isolation processes because conventional implant systems typically have minimum operating voltages in the 20-30 keV range.

One solution to this problem is to implant through a surface layer which acts to move the projected range of the lowest energy implant closer to the semiconductor surface. Titanium is a good choice, since it can be readily removed after the implant step with HF solutions. Moreover, ion mixing effects are not significant until doses $\geq 10^{16}$ cm^{-2}.

Figure 4 shows the calculated ion profiles for the O^+ implant scheme through the Ti over-layer and into the underlying GaN. Note that the projected range of the 30 keV

O^+ implant is now just at the metal-semiconductor interface, effectively reducing the energy of ions reaching the GaN. The calculated vacancy profile is now relatively uniform throughout the doped GaN layer as shown in Figure 5.

The implanted samples were subsequently annealed for 30 secs at temperatures up to 800° C. Figure 6 shows the evolution of the sheet resistance with annealing temperature in the sample implanted without the Ti over-layer. The as-implanted sheet resistance was $8x10^{10}$ Ω/□, and gradually decreased over the entire annealing temperature range. A general rule of thumb for achieving acceptable device isolation is that the implanted region should have a sheet resistance $\geq 10^7$ Ω/□.(1) In this implant process, sheet resistances above this value were achieved for annealing temperatures up to ~650 °C. Note that even for 800 °C anneals, the sheet resistance is still two orders of magnitude above the unimplanted value (10^4 Ω/□).

A similar plot is shown in Figure 7 for the sample implanted with O^+ ions through the Ti over-layer. In this case, a higher maximum sheet resistance was achieved ($4x10^{12}$ Ω/□). This is the highest value reported in GaN. The compensation mechanism is creation of deep electron traps that remove electrons from the conduction band. Upon annealing, some of these damage-related traps are removed, allowing electrons to be returned to the conduction band. The use of the Ti over-layer allows better compensation in the near-surface region and hence a higher as-implanted sheet resistance. The subsequent evolution of the sheet resistance with annealing temperature is similar to the case of implantation without the Ti over-layer , except that the absolute value is larger up to ~600 °C. Secondary Ion Mass Spectrometry (SIMS) measurements on the samples showed that the implanted oxygen did not have any detectable redistribution at 800 °C, consistent with the low diffusivities reported previously.[14]

The sheet resistance of the implanted GaN showed a thermal activation energy of 0.29 eV, as determined by temperature dependent resistance measurements (Figure 8). This gives a rough estimate of the position of the Fermi level in the material. It is somewhat different from the value reported in implanted AlGaN/GaN HFETs (0.71 eV)[12], and is probably at least partially related to the smaller bandgap of the GaN. It is likely that the energy level of traps created in implanted material will depend on the dominant impurities present and on the chemical nature of the implanted species.[1]

Summary and Conclusions

The main conclusions of our study can be summarized as follows:

1. Sheet resistances as high as 4×10^{12} Ω/□ can be achieved in O^+ implanted n-GaN structures when care is taken to ensure ion-induced compensation in the near-surface region by implantation through an over-layer.
2. The sheet resistance remains above 10^7 Ω/□ until annealing temperatures of ~650 °C, which defines the thermal stability of acceptable GaN device isolation.
3. The activation energy of sheet resistance in the O^+ implanted GaN is 0.29 eV. This is well below the desired mid-gap value, but due to the large gap of GaN, the sheet resistance is more than sufficient for device isolation.

Acknowledgements

The work at UF is partially supported by a DARPA/EPRI grant (D. Radack/J. Melcher), contract MDA 972-98-1-0006, monitored by ONR (J. C. Zolper), and by an NSF grant, DMR 97-32865 (L. D. Hess). Sandia is a multi-program laboratory operated by Sandia Corporation, a Lockheed-Martin company, for the US Department of Energy under grant no. DEAC 04-94-AL-85000.

References

1. S. J. Pearton, Mat. Sci. Rep. 4, 313 (1990).
2. M. Orenstein, N. G. Stoffel, A. C. Von Lehmen, J. P. Harbison and L. T. Florez, Appl. Phys. Lett. 59, 31 (1991).
3. K. L. Lear, R. P. Schneider, K. D. Choquette, S. P. Kilcoyne, J. J. Figiel and J. C. Zolper, IEEE Photonic Tech. Lett. 6, 1503 (1994).
4. J. C. Zolper, A. G. Baca and S. A. Chalmers, Appl. Phys. Lett. 62, 2536 (1993).
5. S. J. Pearton, M. P. Ianuzzi, C. L. Reynolds, Jr. and L. Peticolas, Appl. Phys. Lett. 52, 395 (1988).
6. J. C. Zolper, M. E. Sherwin, A. G. Baca and R. P. Schneider, Jr., J. Electron. Mat. 24, 21 (1995).
7. S. C. Binari, H. B. Dietrich, G. Kelner, L. B. Rowland, K. Doverspike and K. D. Wickenden, J. Appl. Phys. 78, 3008 (1995).
8. S. J. Pearton, C. R. Abernathy, P. W. Wisk, W. S. Hobson and F. Ren, Appl. Phys. Lett. 63, 1143 (1993).
9. J. C. Zolper, S. J. Pearton, C. R. Abernathy and C. B. Vartuli, Appl. Phys. Lett. 66, 3042 (1995).
10. S. J. Pearton, C. R. Abernathy, M. B. Panish, R. A. Hamm and L. M. Lunardi, J. Appl. Phys. 66, 656 (1989)
11. J. C. Zolper, S. J. Pearton, C. R. Abernathy and C. B. Vartuli, Mat. Res. Soc. Symp. Proc. 378, 408 (1995).
12. G. Hanington, Y. Hsin, Q. Z. Liu, P. M. Asbeck, S. S. Lau, M. A. Khan, J. W. Yang and Q. Chen, Electron. Lett. 34, 193 (1998).

13. S. J. Pearton, C. R. Abernathy, C. B. Vartuli, J. C. Zolper, C. Yuan and R. A. Stall, Appl. Phys. Lett. 67, 1435 (1995).

14. J. C. Zolper, J. Cryst. Growth 178, 175 (1997).

15. J. M. Van Hove, R. Hickman, J. J. Klaassen, P. P. Chow and P. P. Ruden, Appl. Phys. Lett. 70, 282 (1997).

16. F. Ren, S. J. Pearton, C. R. Abernathy, P. Wisk, T. R. Fullowan, J. Lothian and R. Esaqui, Semicond. Sci. Technol. 8, 413 (1993).

Figure Captions

Figure 1. Schematic of GaN layer structure (top) and scanning electron micrograph (SEM) of TLM pattern (bottom).

Figure 2. Calculated ion profiles in GaN implanted with five separate O^+ implants at energies from 30-325 keV.

Figure 3. Calculated vacancy concentration in GaN implanted with five separate O^+ implants at energies from 30-325 keV.

Figure 4. Calculated ion profiles in a Ti/GaN sample implanted with five separate O^+ implants at energies from 30-325 keV.

Figure 5. Calculated vacancy concentration in a Ti/GaN sample implanted with five separate O^+ implants at energies from 30-325 keV.

Figure 6. Annealing temperature dependence of sheet resistance in O^+ implanted GaN. The implant was performed directly into the GaN.

Figure 7. Annealing temperature dependence of sheet resistance in O^+ implanted GaN. The implant was performed through a Ti over-layer.

Figure 8. Measurement temperature dependence of sheet resistance in O^+ implanted GaN.

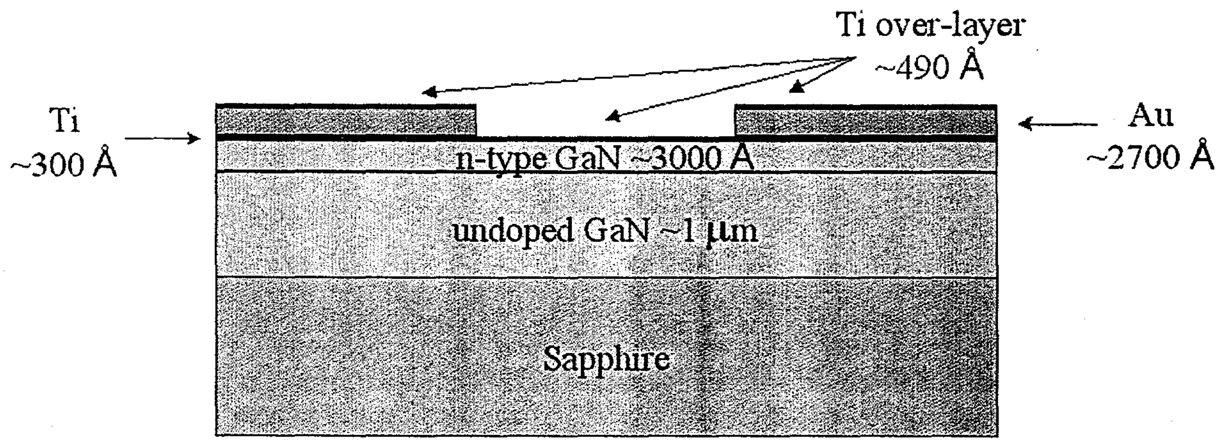
Ti over-layer
~490 Å
Ti
~300 Å
Au
~2700 Å
n-type GaN ~3000 Å
undoped GaN ~1 µm
Sapphire

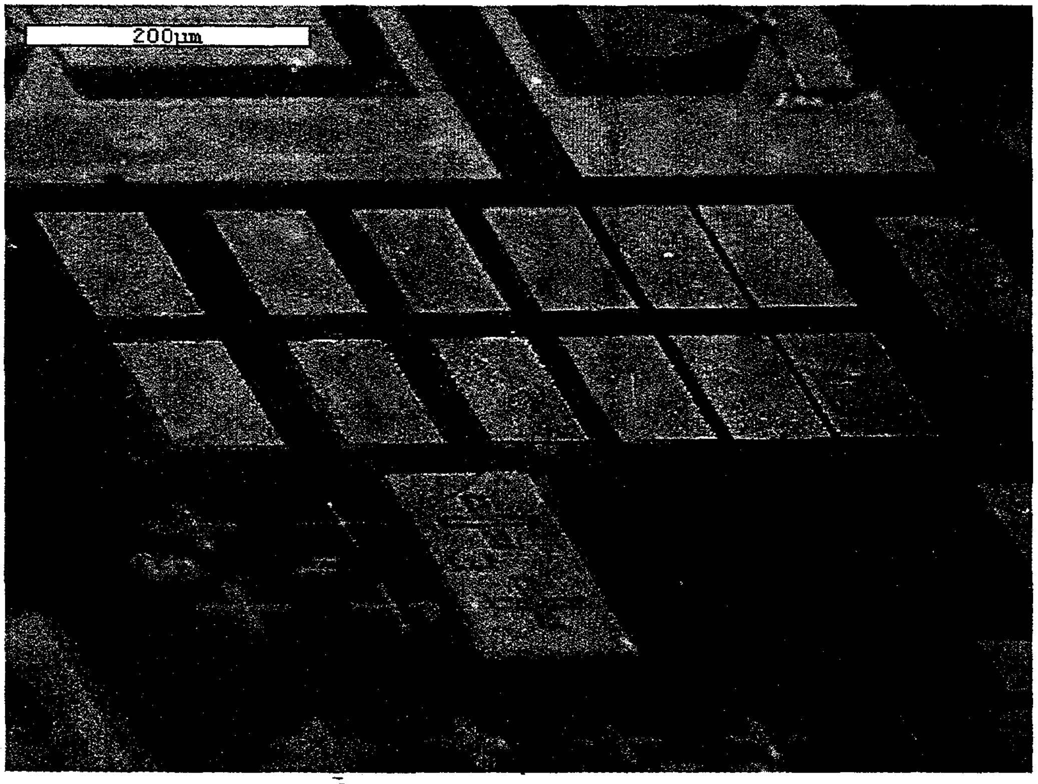
200µm

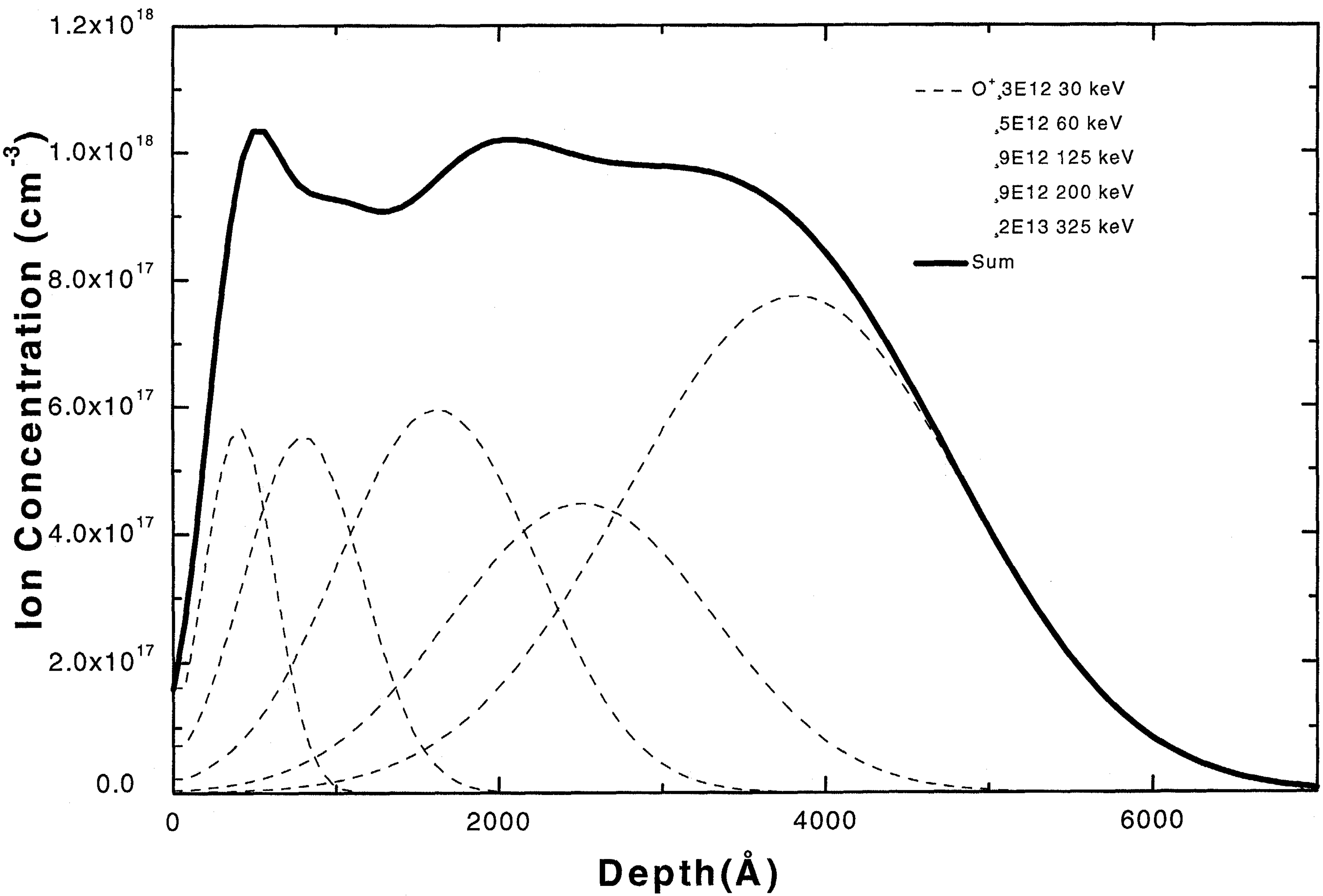

1.2x10^18
1.0x10^18
8.0x10^17
6.0x10^17
4.0x10^17
2.0x10^17
0.0
Ion Concentration (cm^-3)
0
2000
4000
6000
Depth(Å)
O+,3E12 30 keV
,5E12 60 keV
,9E12 125 keV
,9E12 200 keV
,2E13 325 keV
Sum

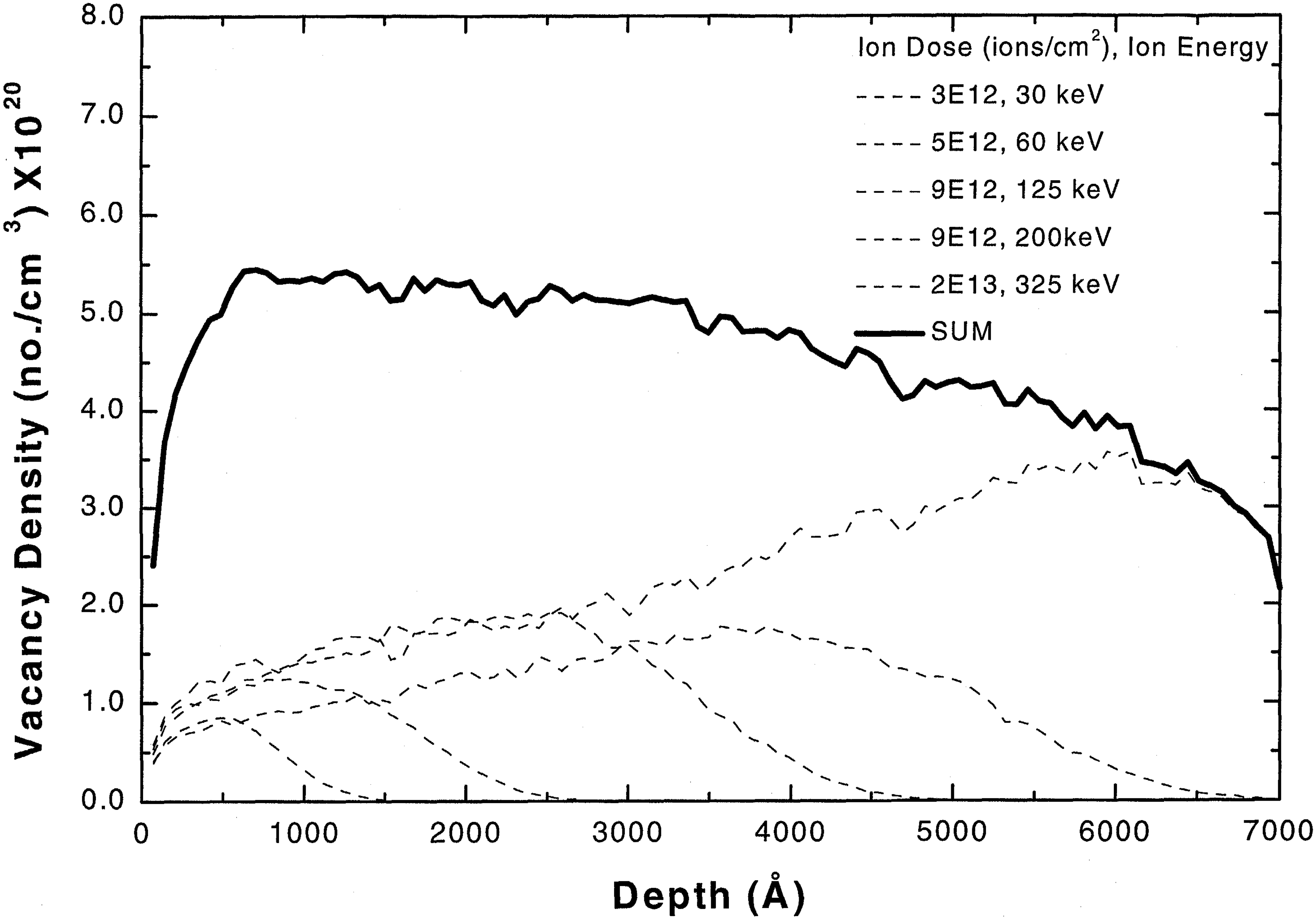
8.0
7.0
6.0
5.0
4.0
3.0
2.0
1.0
0.0
Vacancy Density (no./cm 3) X10 20
0
1000
2000
3000
4000
5000
6000
7000
Depth (Å)
Ion Dose (ions/cm2), Ion Energy
3E12, 30 keV
5E12, 60 keV
9E12, 125 keV
9E12, 200keV
2E13, 325 keV
SUM

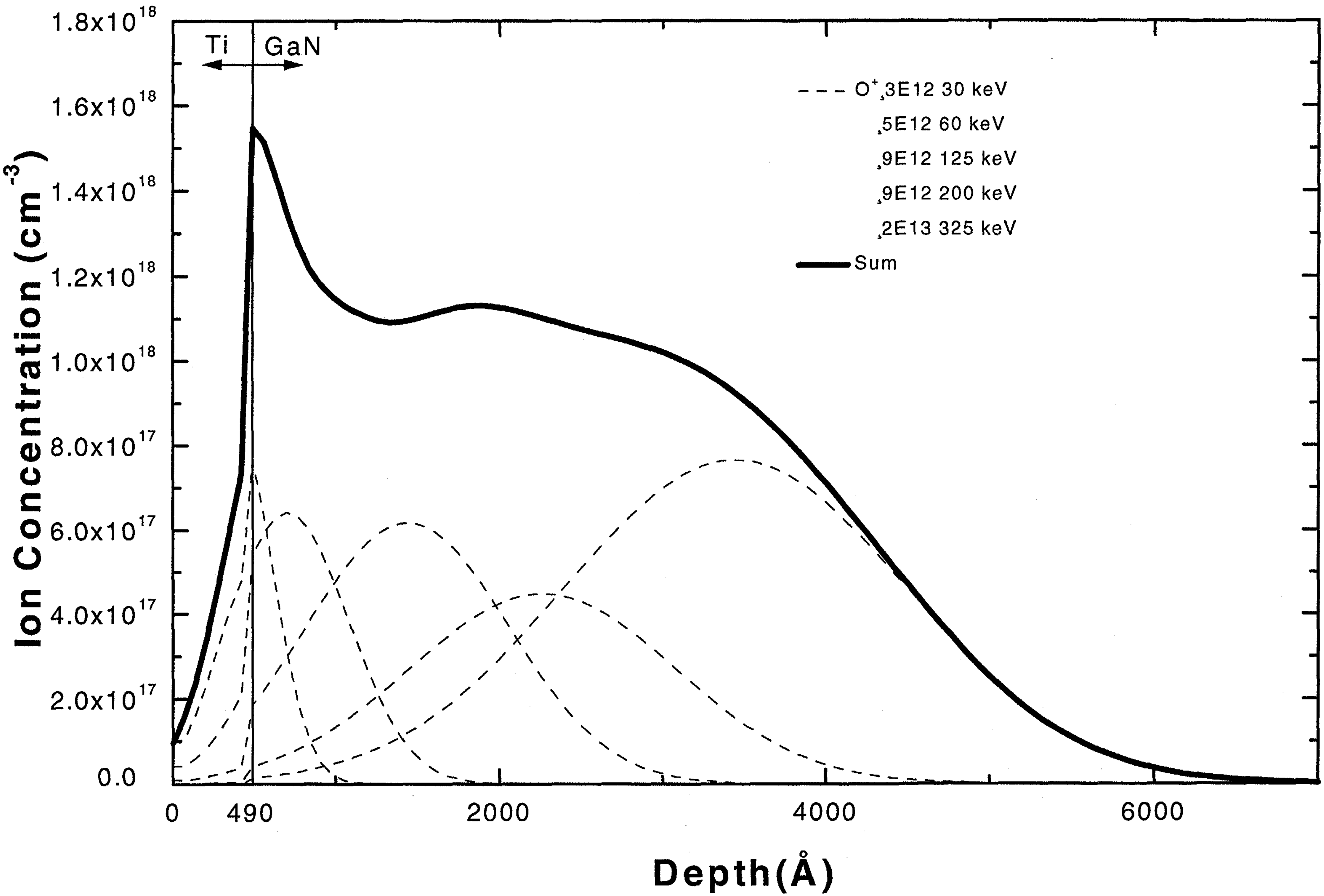

Ti
GaN
O+,3E12 30 keV
,5E12 60 keV
,9E12 125 keV
,9E12 200 keV
,2E13 325 keV
Sum
Ion Concentration (cm-3)
1.8x10^18
1.6x10^18
1.4x10^18
1.2x10^18
1.0x10^18
8.0x10^17
6.0x10^17
4.0x10^17
2.0x10^17
0.0
0
490
2000
4000
6000
Depth(Å)

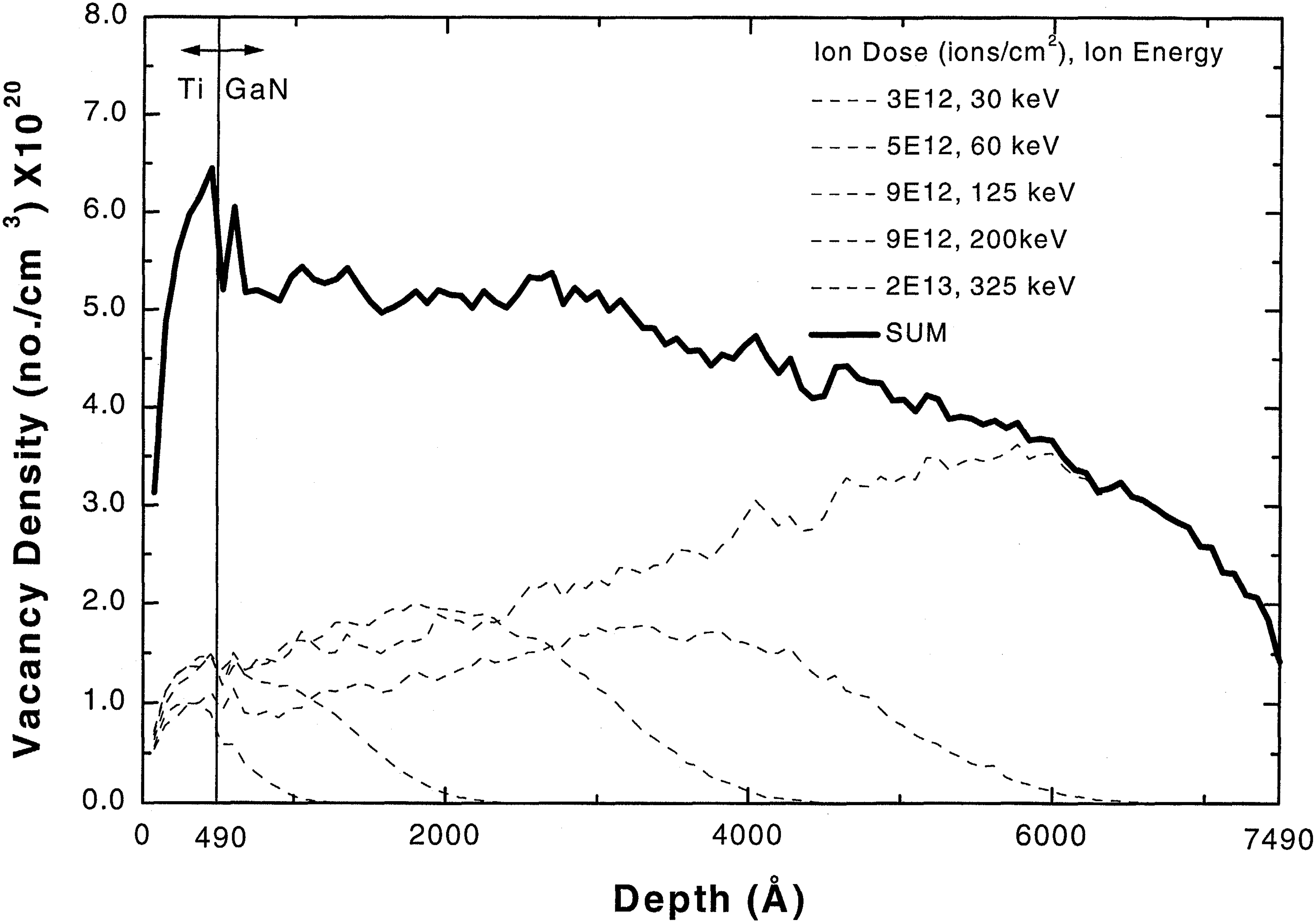

Vacancy Density (no./cm 3) X10 20
Depth (Å)
Ti
GaN
Ion Dose (ions/cm 2), Ion Energy
3E12, 30 keV
5E12, 60 keV
9E12, 125 keV
9E12, 200keV
2E13, 325 keV
SUM
8.0
7.0
6.0
5.0
4.0
3.0
2.0
1.0
0.0
0
490
2000
4000
6000
7490

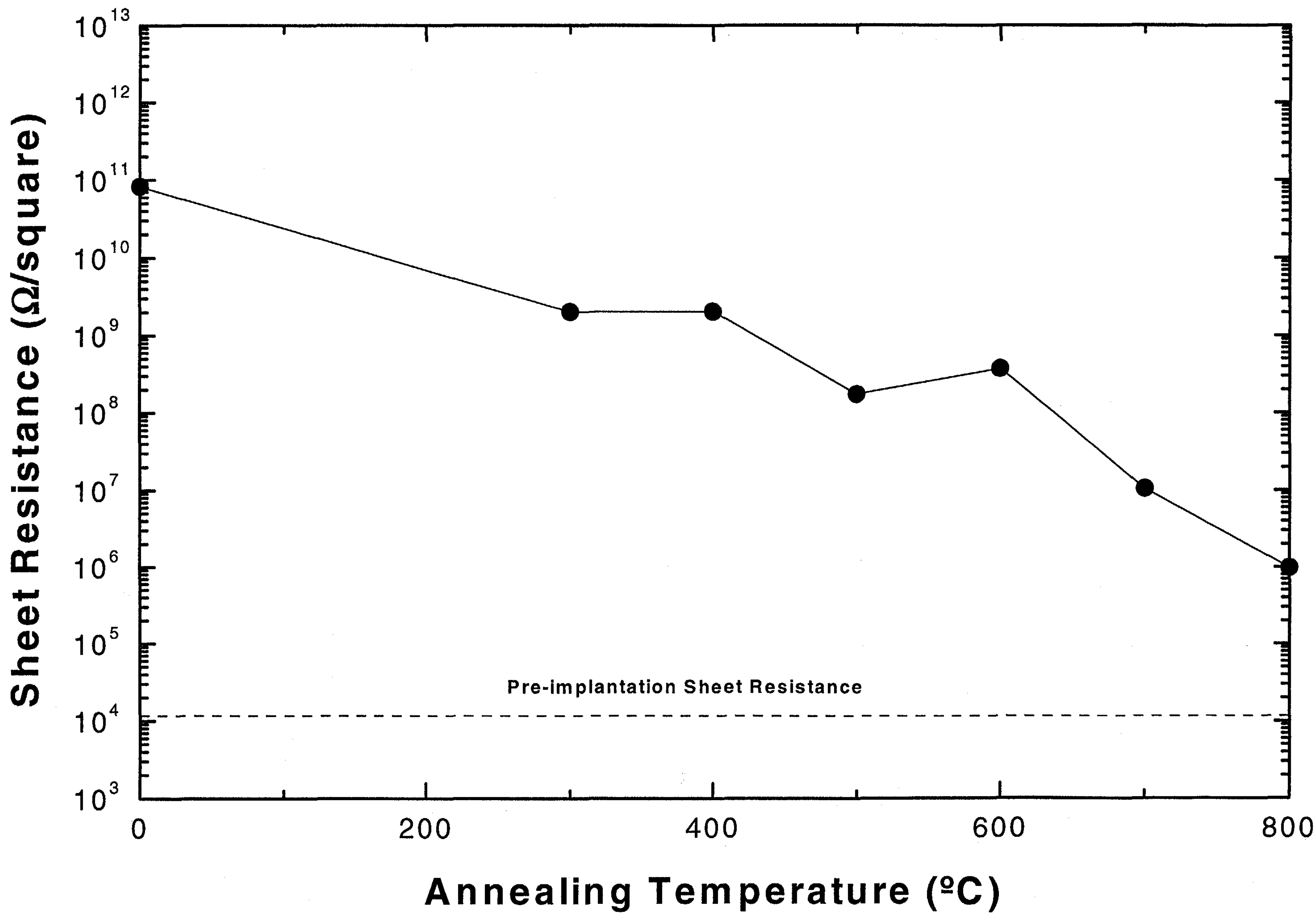
Sheet Resistance (Ω/square)
10^13
10^12
10^11
10^10
10^9
10^8
10^7
10^6
10^5
10^4
10^3
Pre-implantation Sheet Resistance
0
200
400
600
800
Annealing Temperature (ºC)

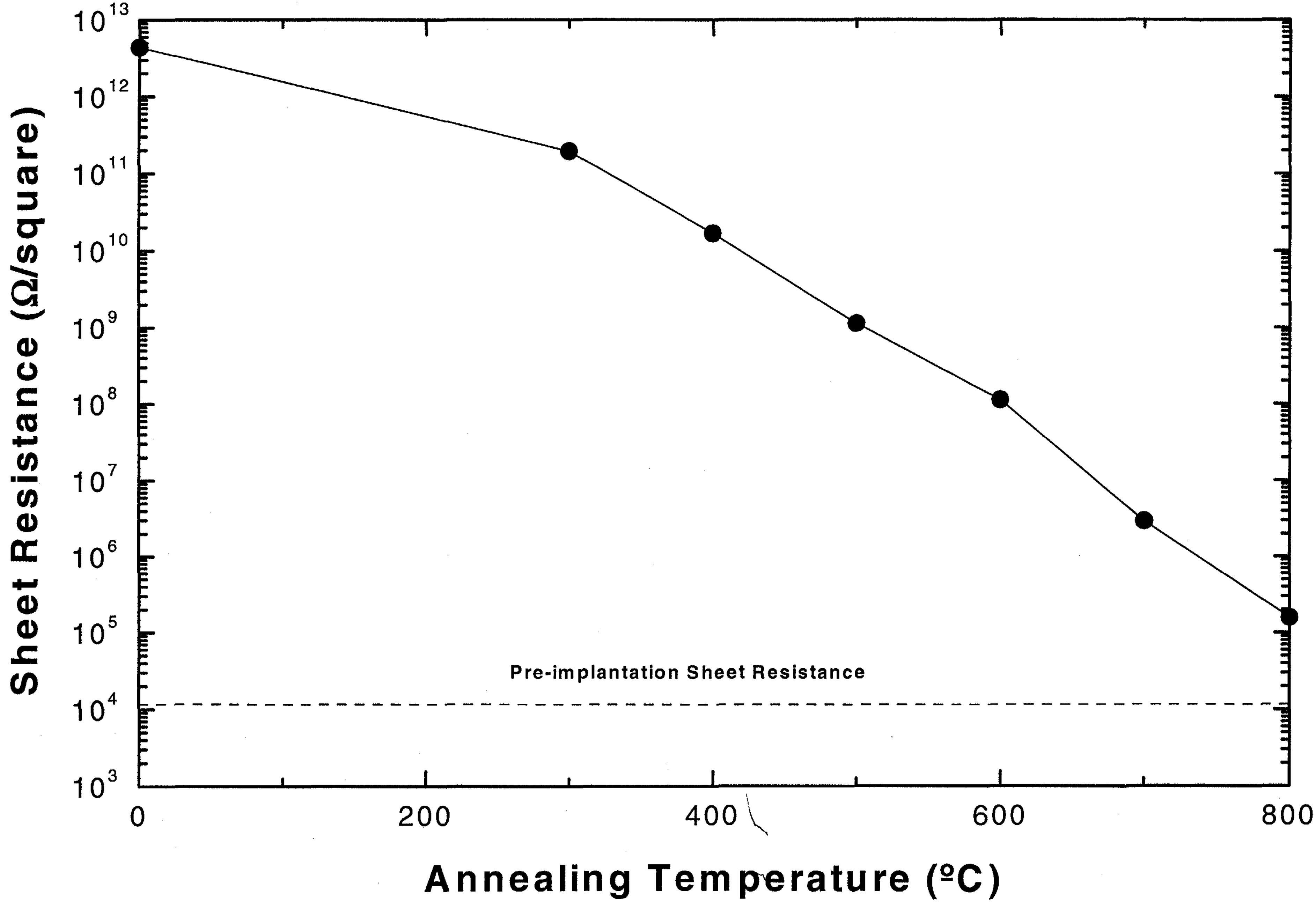

Sheet Resistance (Ω/square)
10^{13}
10^{12}
10^{11}
10^{10}
10^{9}
10^{8}
10^{7}
10^{6}
10^{5}
10^{4}
10^{3}
Pre-implantation Sheet Resistance
0
200
400
600
800
Annealing Temperature (ºC)

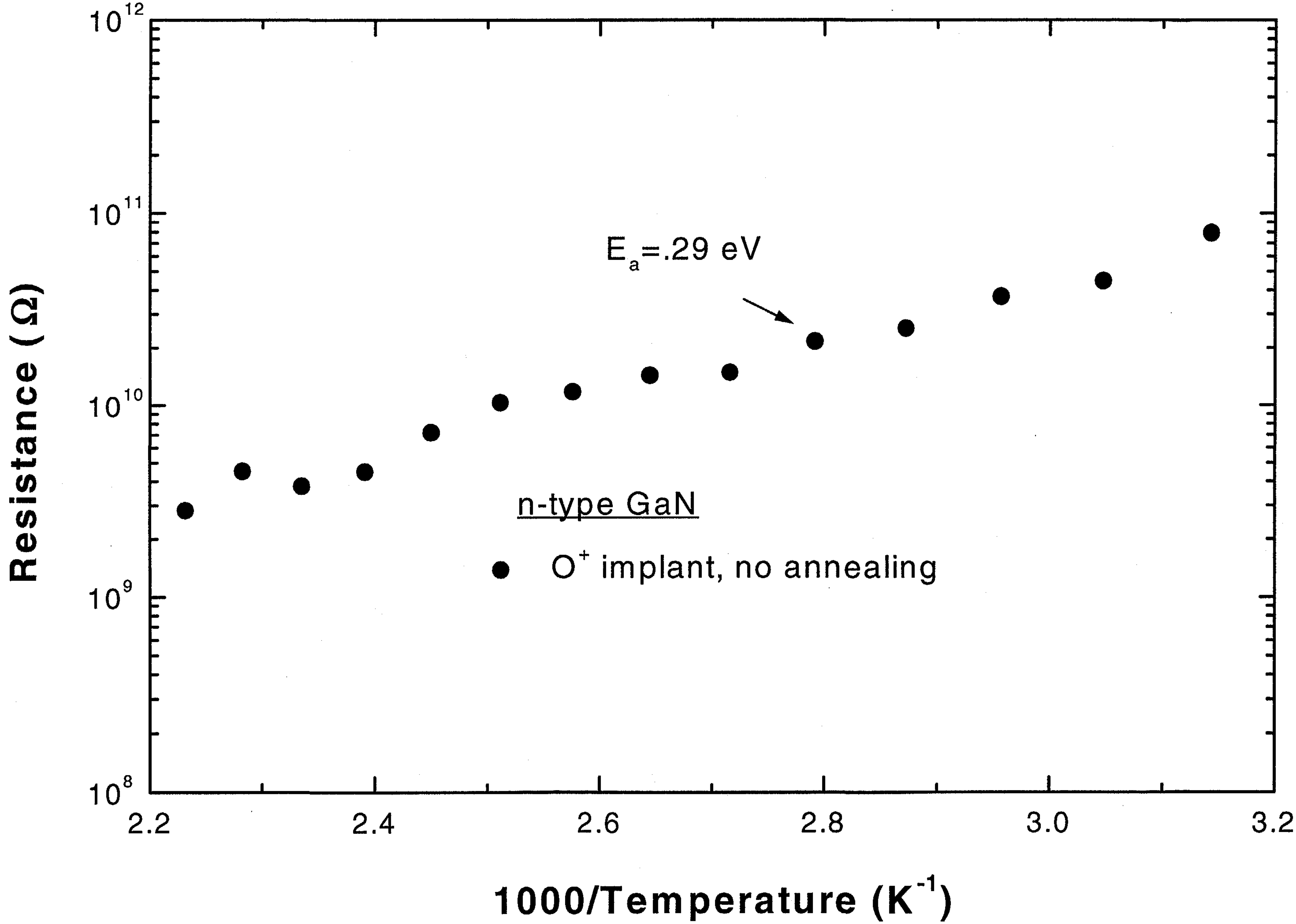

Resistance (Ω)
10^12
10^11
10^10
10^9
10^8
2.2
2.4
2.6
2.8
3.0
3.2
1000/Temperature (K^-1)
E_a=.29 eV
n-type GaN
O^+ implant, no annealing